Functional MRI during Hyperbaric Oxygen: Effects of Oxygen on Neurovascular Coupling and BOLD fMRI signals

Damon P. Cardenas[1,*], **Eric R. Muir**[2,3,*], **Shiliang Huang**[3], **Angela Boley**[4], **Daniel Lodge**[4], and **Timothy Q. Duong**[1,2,3,5]

[1]Graduate School of Biomedical Engineering, University of Texas at San Antonio, San Antonio, TX

[2]Department of Ophthalmology, University of Texas Health Science Center, San Antonio, TX

[3]Research Imaging Institute, University of Texas Health Science Center, San Antonio, TX

[4]Department of Pharmaology, University of Texas Health Science Center, San Antonio, TX

[5]South Texas Veterans Health Care System, Department of Veterans Affairs, San Antonio, TX

Abstract

Hyperbaric oxygen (HBO) therapy is used to treat a number of ailments. Improved understanding of how HBO affects neuronal activity, cerebral blood flow (CBF) and blood-oxygenation-level dependent (BOLD) changes could shed light on the role of oxygen in neurovascular coupling and help guide HBO treatments. The goal of this study was to test two hypotheses: i) activation-induced CBF fMRI response is not dependent on hemoglobin deoxygenation, and ii) activation-induced BOLD fMRI is markedly attenuated under HBO. CBF and BOLD fMRI of forepaw stimulation in anesthetized rats under HBO at 3 atmospheres absolute (ATA) was compared with normobaric air. Robust BOLD and CBF fMRI were detected under HBO. Inflow effects and spin-density changes did not contribute significantly to the BOLD fMRI signal under HBO. Analysis of the T_2^*-weighted signal at normobaric air and 1, 2 and 3ATA oxygen in the tissue and the superior sagittal sinus showed a strong dependence on increasing inhaled $[O_2]$. Spontaneous electrophysiological activity and evoked local-field potentials were reduced under HBO. The differences between normobaric air and HBO in basal and evoked electrical activity could not fully account for the strong BOLD responses under HBO. We concluded that activation-induced CBF regulation in the brain does not operate through an oxygen-sensing mechanism and that stimulus-evoked BOLD responses and the venous T_2^*-weighted signals still have room to increase under 3ATA HBO. To our knowledge, this is the first fMRI study under HBO, providing insights into the effects of HBO on neural activity, neurovascular coupling, tissue oxygenation, and the BOLD signal.

Correspondence: Timothy Duong, PhD, Research Imaging Institute, University of Texas Health Science Center, 8403 Floyd Curl Dr, San Antonio, TX 78229, duongt@uthscsa.edu, Tel 210 567 8100, Fax 210 567 8152.
DPC and ERM contributed equally to this work.

Keywords

forepaw stimulation; CBF; oxygen therapy; BOLD; magnetic susceptibility

INTRODUCTION

Hyperbaric oxygen (HBO) therapy has been used to treat air embolism, decompression sickness, diabetic gangrene, stroke, and traumatic brain injury, among others (Al-Waili et al., 2005). The primary effect of HBO exposure is to increase tissue oxygenation, although there are also secondary effects on: heart rate, respiration rate, blood pCO_2 (Whalen et al., 1965), and basal cerebral blood flow (CBF). Improved understanding of how HBO affects basal and evoked neural activity, CBF and tissue oxygenation could shed light on the role of oxygen in neurovascular coupling, the effects of HBO on blood-oxygenation level dependent (BOLD) signal, as well as guide HBO therapy.

Stimulus-evoked changes in neural activity are known to be tightly coupled to metabolism, cerebral blood oxygenation and CBF under normal physiological conditions. Such neurovascular coupling is modulated by a combination of vasoactive products of metabolism (such as H^+ or adenosine), neurotransmitters, and synaptic signaling (such as K^+ and nitric oxide) (Iadecola, 2004). In addition, it has been suggested that deoxygenated hemoglobin "sensors" could play a role in regulating tissue perfusion (Stamler et al., 1997). It is conceivable that dissolved oxygen in the tissue under HBO (i.e., 3ATA) is sufficient to support a stimulus-evoked increase in oxidative metabolism, obviating the need to increase CBF. The role of oxygen-sensing mechanisms in CBF regulation during increased neural activity, however, has only recently been tested experimentally. Lindauer et al. used HBO to investigate neurovascular coupling in anesthetized rats (Lindauer et al., 2010). Using an open cranial window preparation and laser Doppler flowmetry, they found that the CBF still robustly increased in response to forepaw stimulation during HBO and concluded that activation-induced CBF regulation in the brain does not operate through an oxygen-sensing mechanism. They also reported that the stimulus-evoked deoxyhemoglobin signal detected by intrinsic optical imaging under HBO did not increase, in contrast to the transient increase under normobaric air (NB). The opened skull under HBO could potentially affect tissue oxygen availability on the superficial cortical surface layer, as opposed to deeper cortical layers.

Modern functional MRI techniques (Ugurbil et al., 2000) offer a non-invasive approach to investigate neurovascular coupling by measuring evoked changes in cerebral blood oxygenation and CBF in deep brain structures, enabling further evaluation of the role of oxygen in elevated neuronal activty under HBO. In addition, HBO could have significant effects on the BOLD fMRI signal per se. Because venous pO2 is likely nearly or fully saturated under HBO, it is unknown if stimulation could evoke a BOLD fMRI signal under HBO. Multimodal fMRI has the potential to provide valuable information regarding the effects of HBO on neural activity, neurovascular coupling, tissue oxygenation, and the BOLD fMRI signals. Muir et al. recently constructed an MRI-compatible hyperbaric chamber for use in an animal MRI scanner, which they used to investigate the effects of

HBO on the MR signal characteristics (Muir et al., 2014). They found that 4ATA HBO decreased brain T_1, attributed to increased dissolved oxygen, but increased T_2 and T_2^* attributed to the BOLD effect from increased hemoglobin oxygen saturation.

The goal of this study was to utilize this MRI-compatible HBO chamber to test two hypotheses: i) activation-induced CBF fMRI response is not dependent on hemoglobin oxygenation, and ii) activation-induced BOLD fMRI is markedly attenuated under HBO. CBF and BOLD fMRI of forepaw stimulation in anesthetized rats was performed under 3ATA HBO and compared with normobaric air (NB). Additional experiments were performed to evaluate the potential contributions of stimulus-evoked inflow, spin density, and electrical activity to BOLD fMRI responses under HBO. Baseline T_2^*-weighted MRI signals were analyzed in the primary somatosensory cortex (S1) and superior sagittal sinus (SSS) for NB and multiple HBO conditions.

2. METHODS

Hyperbaric Chamber

A custom-made hyperbaric chamber for rodent MRI scanners consisted of an animal cradle placed into a PVC pipe with O-rings on both ends of the cradle to provide a tight seal as described previously (Muir et al., 2014). The chamber was pressure tested with water up to 5ATA. HBO was achieved using ambient air to pressurize the chamber with a separate line to deliver oxygen locally to the nose. This protocol prevents the risk of explosion associated with highly concentrated oxygen. We have previously measured the O_2 percentage of our setup and found the O_2 readings were 90%–93% (Muir et al., 2013). Note that this was made using a small tube inserted to sample the gas in the outlet of the nose cone outside the MRI scanner because the gas needed to be sampled at low flow rates to maintain hyperbaric pressure in the chamber.

Cables for biometric equipment (temperature probe and pulse oximeter), polyethylene tubing for delivery of intravenous anesthesia, and electrodes for forepaw stimulation were passed through a hole in one of the endplates and sealed with silicone sealant. Animal temperature was maintained with circulating warm water through a winding of rigid plastic tubing. The chamber was pressurized in 10 min at an average rate of 0.2ATA per minute to prevent potential side effects from rapid pressurization. Sustained HBO exposure was limited to about 25 min, by switching back to air delivery through the line to the nose, to avoid potential O_2 toxicity.

Animal preparation

Animal experiments were approved by the local Institutional Animal Care and Use Committee. Five groups of experiments were performed on male Sprague-Dawley rats (325 ± 50 g): (I) the main experiment involving simultaneous BOLD and CBF fMRI under NB and HBO (3ATA) (n = 8), (II) variable TR BOLD fMRI experiments under HBO (n = 3), (III) variable TE BOLD fMRI experiments under HBO (n = 3), (IV) T_2^*-weighted MRI signal changes during NB, normobaric oxygen, and 2 and 3ATA HBO (n = 3), and (V) electrophysiological experiments outside the MRI scanner under NB and HBO (n = 7).

Rats were initially anesthetized using 5% isoflurane and maintained at 2% isoflurane during preparation. Animals were placed into a head holder with ear and tooth bars and secured into the cradle. The animals were sealed inside the chamber and placed into the MRI scanner. The anesthetic was then switched to α-chloralose (a bolus of 60 mg/kg I.V. followed by 30 mg/kg/hr after 45 mins).

The rats were imaged under spontaneous breathing conditions. Respiration, heart rate, and arterial oxygen saturation were monitored (MouseOx, STARR Life Science Corp., Oakmont, PA), and rectal temperature was maintained at $37 \pm 0.5°$ C with a feedback-regulated circulating warm water pad. Needle electrodes were inserted in both forepaws between digit 2 and 4, connected in series. Both forepaws were stimulated simultaneously (2 mA, 3 Hz, 0.3 ms) (Shen et al., 2005; Sicard and Duong, 2005) using a paradigm of four repeats of 30-s stimulation and 96-s rest periods.

MRI Acquisition

MRI was performed on a 7T magnet with 400 mT/m gradients (Bruker, Billerica, MA). A surface coil (2 cm diameter) was used for brain imaging and a neck coil for perfusion labeling (Duong et al., 1999; Shen et al., 2003; Shen et al., 2005). Coil-to-coil electromagnetic interaction was actively decoupled. Global shimming was only performed once at the beginning of a session.

For Group I, simultaneous and combined BOLD and CBF fMRI measurements were made using the continuous arterial spin-labeling technique with single-shot, gradient-echo, echo-planar-imaging acquisition. Paired images were acquired alternately – one with arterial spin labeling and the other without (control). Non-labeled images were used for BOLD fMRI analysis. MRI parameters were: TR = 3 s, nominal flip angle = 90°, TE = 20 ms, FOV = 25.6x25.6 mm, matrix = 96x96, and seven 1.5-mm thick slices. Evoked fMRI was acquired twice per animal at each condition.

For Group II, BOLD fMRI was acquired similarly as in Group I, but without ASL, using TR = 3 and 10 s. For Group III, BOLD fMRI was acquired similarly as in Group I, but without ASL, with TR = 10 s, using TE = 20, 30, and 40 ms. For both groups II and III, evoked BOLD fMRI was acquired twice per animal at each set of parameters.

For Group IV, to evaluate of the effects of HBO on the baseline T_2^*-weighted MRI signal, MRI was acquired continuously from NB, to normobaric oxygen, to 2ATA HBO, and to 3ATA HBO. MRI acquisition was similar to group I but without ASL.

MRI Analysis

Image analyses were performed using Matlab (MathWorks, Natick, MA), Statistical Parametric Mapping 5 (SPM5), and STIMULATE (University of Minnesota, Minneapolis, MN). Preprocessing of data consisted of image alignment using SPM5 followed by averaging of the repeated trials in each animal. No spatial or temporal smoothing was applied. For fMRI analysis, non-labeled images were used for BOLD analysis, and CBF was calculated (Shen et al., 2005; Sicard and Duong, 2005). CBF and BOLD percent changes due to stimulation were tabulated for 6x6 pixels regions of interest (ROIs) encompassing the

forepaw primary somatosensory cortices (S1). The ROIs were centered based on anatomical location (not fMRI maps) at 3.4mm lateral to the longitudinal fissure and 2 mm superior to the corpus callosum in each hemisphere to avoid bias. The same ROIs were used for each animal across different measurements and were manually corrected for shift along the phase-encoding direction in the image due to the HBO condition (Muir et al., 2014). Normalized absolute signal intensities to the baseline normobaric air conditions were tabulated for individual animals. Percent-change activation maps between control and stimulation periods were calculated in STIMULATE.

T_2^*-weighted MRI signals under NB, 1, 2 and 3ATA oxygen were analyzed in ROIs encompassing the S1 (as described above) and the SSS. HBO conditions. Ratios of HBO to NB images were calculated pixel-by-pixel for comparison.

Electrophysiology

In Group V, to implant electrodes, rats were pretreated with atropine (0.1 mg/kg i.p.), anesthetized with sodium pentobarbital (60 mg/kg i.p.) and placed in a stereotaxic apparatus using atraumatic ear bars. A bur hole was drilled overlying the S1 region of the cortex (4 mm lateral and 1mm caudal to bregma) on the left hemisphere of the rat and a 0.2 mm diameter stainless steel electrode (Plastics1: MS303/2-AIU) was lowered into S1 cortex to a depth of 2 mm from the surface of the skull. The ground wire was looped around one of the stainless steel screws that secured the electrode to the skull using dental cement. After implantation, rats were treated with ketoprofen (5 mg/kg SQ) and given two weeks to recover.

For recording, α-chloralose anesthesia was used as in the MRI experiments. The recording electrode was connected to the headstage of an extracellular amplifier (Model 2400B, Dagan Corp, Minneapolis, MN). Spontaneous local field potentials were recorded form the S1 cortex under NB and HBO conditions Following 10 mins of spontaneous recordings, the forepaws were stimulated using the paradigm detailed above and evoked S1 local field potentials were recorded. Data were acquired at 1 kHz and filtered (low cutoff: 1 Hz, high cutoff 100 Hz) (Powerlab ML866, ADI Instrument, Colorado Spring, CO). To quantify spontaneous oscillatory activity, segments of data were analyzed by Fourier transform algorithm (Hamming with 8k FFT size) and power across distinct frequency bands was compared between NB and HBO conditions. To examine evoked potentials, the magnitude of the first negative peak was recorded and compared between NB and HBO conditions.

Statistical Analysis

Group-average data are expressed as mean ± standard error of the mean (SEM) unless indicated otherwise. Paired t-tests were used to identify statistical significance. $P < 0.05$ was taken as statistically significant.

3. RESULTS

HBO increased arterial oxygenation and decreased respiration rate

Table 1 summarizes the respiration rate, heart rate, and arterial blood oxygen saturation under NB and HBO from 11 out of 22 rats. Respiration rate and arterial oxygen saturation were statistically different between NB and HBO as expected. Heart rate trended lower but did not reach statistical significance.

Robust BOLD and CBF fMRI responses detected under 3ATA HBO

Normalized T_2^*-weighted (BOLD) signals from the primary somatosensory cortices from non-stimulated and stimulated periods during HBO and NB are shown Figure 1. Under non-stimulated condition, the normalized absolute T_2^*-weighted signal intensities were statistically higher under HBO compared to NB ($P < 0.05$) as expected. Forepaw stimulation reliably evoked BOLD fMRI responses in the bilateral primary somatosensory cortices under both NB and HBO. There were, however, no statistical differences in BOLD evoked percent changes between the NB and HBO conditions.

Forepaw stimulation also reliably evoked CBF fMRI responses in the bilateral primary somatosensory cortices under both NB and HBO (Figure 2). There were however, no statistical differences in CBF evoked percent changes between the NB and HBO conditions.

Inflow effect did not contribute significantly to BOLD under HBO

To evaluate the possible contribution of inflow effect to the BOLD fMRI response under HBO, experiments were also performed with 10 s TR (Figure 3A). The BOLD response with 10 s TR was not statistically different from that with 3 s TR. This result indicates that inflow effects did not significantly contribute (0.5% of the 3% change) to the observed BOLD fMRI response under HBO.

Spin-density changes did not contribute to the BOLD response under HBO

To evaluate the possible contribution of spin-density changes to the BOLD fMRI response under HBO, experiments were performed with varbiable TE (Figure 3B). The BOLD change when extrapolated to TE = 0 was close to zero (0.3%). This result indicated that spin-density effects did not substantially contribute to the BOLD fMRI response under HBO.

Veneous oxygen saturation did not saturate under 3ATA HBO

To determine whether the BOLD fMRI signal was saturated at 3ATA HBO, T_2^*-weighted MRI signal at NB, normobaric oxygen, and at 2 and 3ATA HBO was acquired (Figure 4). The ratio of HBO to NB images showed hyperintensities in brain regions consistent with venous vessels such as the superior sagittal sinus (SSS, arrow). Hyperintensities were also evident on large surface venous vessels (arrowheads). T_2^*-weighted MRI signals from the S1 and SSS showed strong dependence on increasing inhaled $[O_2]$. The signal changes were markedly larger in the venous blood in the SSS compared to S1 due to the difference in cerebral blood volume. The image contrast between SSS and surrounding brain tissue decreased with increasing inhaled $[O_2]$. The T_2^*-weighted MRI signals of the cortex and especially the SSS were still increasing up to 3ATA HBO.

Basal and stimulus-evoked electrical activity is reduced under HBO

To evaluate the possible contribution of differences in neural activity to the BOLD fMRI response under HBO, electrophysiolgoical experiments under baseline and stimulated conditions were performed (Figure 5). Under baseline conditions, spontaneous electrical activity was overall slightly lower under HBO compared to NB. Analysis of different frequency bands of the spontaneous electrical activity showed that spontaneous activities of the theta, alpha, beta and gamma bands were statistically different between HBO and NB, but not the delta band. Under stimulated conditions, electrical activity measured by local field potential was significantly lower under HBO compared to NB (Figure 6).

4. DISCUSSION

Effects of HBO on physiological parameters

Arterial blood oxygen saturation increased significantly, respiration rate decreased significantly, and heart rate trended lower under HBO compared to NB. Mild reductions in respiration and heart rate are consistent with human physiological data under HBO (Whalen et al., 1965), and with rat physiological data under normobaric oxygen (Sicard and Duong, 2005). Reduced respiration leads to mild hypercapnia under normobaric oxygen (Duong et al., 2001; Sicard and Duong, 2005), which should increase basal CBF. However, oxygen also has vasoconstrictive effects, which should decrease basal CBF. These two opposing effects could cancel each other. Sicard et al. previously reported basal CBF under normobaric oxygen to be slightly higher than NB (Sicard and Duong, 2005). We predict that CBF under HBO is slightly lower than NB. However, we did not report quantitative CBF in this study because HBO could potentially affect arterial blood and tissue T_1 due to the large quantity of dissolved paramagnetic oxygen, confounding quantification somewhat. Further study is needed to accurately quantify CBF under HBO with MRI. Relative stimulus-evoked CBF changes, however, shoud not be sigificantly affected by altered T_1.

Stimulus-evoked neurovascular coupling is not driven by blood oxygen availability

Robust and strong stimulus-evoked CBF fMRI response was detected under HBO that was not statistically different from that under NB. These results indicate that activation-induced CBF regulation in the brain does not operate through an oxygen-sensing mechanism. This finding is consistent with Lindauer et al. who investigated the effect of HBO (3 and 4ATA) on neurovascular coupling using laser Doppler flowmetry in anesthetized rats (Lindauer et al., 2010). They found that during HBO, forepaw stimulation robustly increased CBF and concluded that activation-induced CBF regulation in the brain did not operate through the release of vasoactive mediators based on hemoglobin deoxygenation or through a tissue-based oxygen-sensing mechanism.

Signal sources of the BOLD fMRI signals under HBO

Contrary to our hypothesis, strong stimulus-evoked BOLD fMRI response was detectable under HBO that was not statistically different from that under NB. There are a few potential explanations for this finding. The BOLD fMRI response under HBO could come from: i) inflow effect due to use of insufficiently long TR, ii) spin-density increase due to stimulus-

evoked increase in cerebral blood volume, iii) differences in evoked electrophysiological activity between HBO and NB, and/or iv) hemoglobin oxygenation changes.

To evaluate possible inflow effect, BOLD fMRI with different TRs was performed. There was no statistically significant difference between data acquired at 3 s and at 10 s. We concluded that at most the inflow effect contributed ~0.5% of the total 3% BOLD signal changes under HBO.

To evaluate possible spin-density effects, BOLD fMRI was performed with different TEs to extrapolate the fMRI response at TE = 0 ms. This finding showed that the spin-density contribution to the evoked BOLD fMRI changes under HBO was negligible.

To evaluate possible contribution to the BOLD responses from differences in evoked neural activity between HBO and NB, we performed evoked potential measurements associated with forepaw stimulation. We found that the evoked potentials under HBO were significantly smaller than that under NB. This is consistent with the finding that evoked cerebral oxygen consumption decreased slightly under normobaric hyperoxia and increased slightly under hypoxia compared to air in humans (Xu et al., 2012) and in animals (Sicard and Duong, 2005). It is possible that more energy is needed to sustain homeostatis under hypoxia because anaerobic metabolism is less efficient whereas less energy is needed to sustain homeostatis under hyperoxia. In contrast, Lindauer et al. reported that the evoked potentials due to forepaw stimulation were not statistically different between HBO and NB. Under HBO, a decrease in evoked neural activity with the corresponding unchanged evoked CBF response could possibly lead to an increased BOLD fMRI response. Possible differences are that we used higher current amplitude and a longer stimulation period with a shorter rest period. The decrease in evoked potential may be a reflection of desensitization or fatigue of the neurons. Further investigation is needed.

Taken together, these findings indicated that the effects of stimulus-evoked changes in inflow, spin-density, and neural activity are unlikely to completely account for the observed stimulus-evoked increases in BOLD fMRI signals under HBO.

There is still room for T_2^*-weighted MRI signal to increase under 3ATA HBO

To further corroborate the contribution of oxygenation changes to the BOLD fMRI increase under HBO, the ratio of NBO to NB T_2^*-weighted images showed relatively hyperintense regions consistent with large venous structures such as the SSS and the surface venous vessels, while the overall brain showed relatively uniform intensity. T_2^*-weighted signal intensities of the SSS and S1 were also quantified as a function of increasing inhaled $[O_2]$, from NB, normobaric oxygen, and at 2 and 3ATA HBO. The signal contrast between the SSS and surrounding tissue decreased with increasing $[O_2]$. The T_2^*-weighted MRI signal intensities in the SSS and S1 increased ~250% and 12%, respectively, when transitioned from NB to 3ATA HBO. The smaller increase in the cortex is expected because of the small venous blood volume fraction in tissue. The T_2^*-weighted MRI signal intensity in the cortex, and especially SSS, were still increasing up to 3ATA HBO. These data indicated that T_2^*-weighted signals in veins (and likely capillaries) still have room to increase under 3ATA HBO.

We estimated the arterial pO2 required to eliminate the need for O_2 bound to hemoglobin to support metabolism, and thus eliminate all deoxyhemoglobin. Under normoxia ($PaO_2 = 100$ mmHg), hemoglobin in the arterial blood is fully saturated and carries ~9 mM of O_2, whereas the plasma carries about 1.5% of total (0.135 mM) (Duong et al., 2001). For a typical brain O_2 extraction fraction of 50% (Magata et al. 2003), the dissolved gas concentration extracted from the blood would need to be 4.5 mM or 33 times of normobaric normoxia (or 3300 mmHg) to support metabolism. The ambient oxygen level at 3 ATA HBO (2280 mmHg) would not completely eliminate deoxyhemoglobin. Thus, there is likely still some deoxyhemoglobin in the venous side, consistent with the observation that T_2^*-weighted MRI signals leveled off substantially but not completely (Figure 4).

Note also that while tissue T_2^* is lengthened by increasing O_2 at normoxic pO2 due to hemoglobin, after hemoglobin is fully saturated the dissolved O_2 could shorten T_2^*. Our data at 3 ATA HBO (Figure 4) showed that T2*-weighted MRI signals in the cortex and the super sagittal sinus did not pass the point of full hemoglobin saturation. Future studies will investigate beyond 3 ATA HBO.

Our findings however are inconsistent with blood-gas measurements under HBO in awake humans (Whalen et al., 1965) where they found that the venous oxygenation under air, normobaric oxygen, and 3ATA HBO were 41, 57, 424 mmHg, corresponding to 75, 87 and 100% O_2 saturation, respectively (the arterial oxygenation under air, normobaric oxygen, and 3ATA HBO were 89, 507 and 1721 mmHg, corresponding to 96, 100 and 100% arterial blood O_2 saturation, respectively, as expected). Venous pO2 was sampled at the junction of the superior vena cava and the right atrium, which might differ from the SSS. To our knowledge, there are no other venous blood-gas measurements under HBO in animals or humans. There are several potential explanations for this apparent discrepancy: (I) Oxygen extraction fraction in the brain is higher compared to other parts of the body, and thus the venous blood in the brain under HBO would have less oxygen content compared to the vena cava. If this were the case, we predict that T_2^*-weighted MRI signals in muscle, where oxygen extraction fraction is lower, would saturate at lower $[O_2]$ and stimulation of muscle would result in negligible or markedly attenuated BOLD responses under HBO. Direct pO2 measurement in the jugular vein under HBO would also be helpful in addressing this apparent discrepancy. (II) Capillary blood pO_2 is lower than venous blood pO2 because of oxygen extraction and/or possible shunting of vessels, and thus could contribute to the BOLD fMRI response under HBO. (III) Human blood-gas data were obtained from awake conditions whereas our rat data were from anesthesia. Under anesthesia, tissue is likely less oxygenated because of depressed cardiovascular function, likely resulting in lower venous blood pO2 and allowing a stimulus-evoked BOLD fMRI response under HBO. There could also be species differences although less likely. Further investigation into these potential contributing factors is needed.

Our finding is incongruent with Lindauer et al. who reported (Lindauer et al., 2010) that the stimulus-evoked deoxyhemoglobin signal detected by intrinsic optical imaging under HBO did not change, whereas that under NB increased transiently. Their result suggests that blood oxygenation is fully saturated under HBO. In contrast, we found the stimulus-evoked BOLD fMRI signals remained strong under HBO, and the T_2^*-weighted signal of SSS did not

appear to saturate under 3ATA HBO. This apparent discrepancy could be due to the use of open skull preparation under HBO in their study, which could potentially enhance tissue oxygen delivery because the superficial cortical tissue may be more exposed to the ambient HBO. It is also possible that there are differences in the functional CBF responses from the superficial cortical layers (Doppler) and the deeper cortical layers (fMRI). Another possible explanation is that the deoxyhemoglobin signal detected by intrinsic optical imaging is largely localized to small vessels, whereas the T_2^*-weighted signals came from larger vessels, including venules and veins. Further investigation is needed.

Spontaneous activity under NB and HBO

It is interesting to note that spontaneous activity under HBO is reduced compared to NB. Spontaneous activities of the theta, alpha, beta and gamma bands decreased under HBO compared to NB, while the delta band showed a decreasing trend but did not reach statistical significance. Previous studies have reported reduced oxygen consumption in brain slices (Mulkey et al., 2001) and reduced glucose consumption in the pig brain in vivo (van Hulst et al., 2003), but no changes in delta and theta band activity in humans (Litscher et al., 1990) under HBO. These differences could be due to difference in species and/or anesthesia. Nonetheless, these data clearly demonstrated that HBO conditions do not induce generalized increases in evoked cortical activity and thus differences in neural activity is unlikely to contribute to significant BOLD fMRI responses under HBO.

5. CONCLUSION

CBF and BOLD fMRI under HBO offers a means to evaluate the role of oxygen in neurovascular coupling as well as the effects of hyperbaric oxygen on basal and evoked BOLD and CBF signals. Our data support the hypothesis that activation-induced CBF regulation in the brain does not operate through an oxygen-sensing mechanism and that stimulus-evoked BOLD responses and venous T_2^*-weighted MRI signals still have room to increase under 3ATA HBO.

Acknowledgments

Abbreviations

HBO	hyperbaric oxygen
NB	normobaric air
ATA	atmospheres absolute
BOLD	blood oxygen level dependent
SEM	standard error of the mean
SD	standard deviation
EEG	Electroencephalography

S1	primary somatosensory cortex
SSS	superior sagittal sinus
ROI	region of interest
CBF	cerebral blood flow

References

Al-Waili NS, Butler GJ, Beale J, Abdullah MS, Hamilton RW, Lee BY, Lucus P, Allen MW, Petrillo RL, Carrey Z, Finkelstein M. Hyperbaric oxygen in the treatment of patients with cerebral stroke, brain trauma, and neurologic disease. Adv Ther. 2005; 22:659–678. [PubMed: 16510383]

Duong TQ, Iadecola C, Kim SG. Effect of hyperoxia, hypercapnia, and hypoxia on cerebral interstitial oxygen tension and cerebral blood flow. Magn Reson Med. 2001; 45:61–70. [PubMed: 11146487]

Duong, TQ.; Silva, AC.; Lee, S-P.; Kim, S-G. International Soc Magn Reson Med. Philadelphia, PA: 1999. Comparison of Spatial Localization between Synaptic Activity and Hemodynamic Responses following Somatosensory Stimulation: an MRI study at 9.4 Tesla.

Iadecola C. Neurovascular regulation in the normal brain and in Alzheimer's disease. Nat Rev. 2004; 5:347–360.

Lindauer U, Leithner C, Kaasch H, Rohrer B, Foddis M, Fuchtemeier M, Offenhauser N, Steinbrink J, Royl G, Kohl-Bareis M, Dirnagl U. Neurovascular coupling in rat brain operates independent of hemoglobin deoxygenation. J Cereb Blood Flow Metab. 2010; 30:757–768. [PubMed: 20040927]

Litscher G, Friehs G, Maresch H, Pfurtscheller G. Electroencephalographic and evoked potential monitoring in the hyperbaric environment. J Clin Monit. 1990; 6:10–17. [PubMed: 2295893]

Magata M, Temma T, Iida H, Ogawa M, Mukai T, Iida Y, Morimoto T, Konishi J, Saji H. Development of Injectable O-15 Oxygen and Estimation of Rat OEF. J Cereb Blood Flow Metab. 2003; 23:671–676. [PubMed: 12796715]

Muir ER, Cardenas D, Huang S, Roby J, Li G, Duong TQ. MRI under hyperbaric air and oxygen: Effects on local magnetic field and relaxation times. Magn Reson Med. 2014; 72:1176–1181. [PubMed: 24243603]

Mulkey DK, Henderson RA 3rd, Olson JE, Putnam RW, Dean JB. Oxygen measurements in brain stem slices exposed to normobaric hyperoxia and hyperbaric oxygen. J Appl Physiol (1985). 2001; 90:1887–1899. [PubMed: 11299283]

Posse S, Wiese S, Gembris D, Mathiak K, Kessler C, Grosse-Ruyken ML, Elghahwagi B, Richards T, Dager SR, Kiselev VG. Enhancement of BOLD-contrast sensitivity by single-shot multi-echo functional MR imaging. Magn Reson Med. 1999; 42:87–97. [PubMed: 10398954]

Russell GB, Vance WT, Graybeal JM. Attenuation of midazolam-induced EEG activation in rats by both flumazenil and hyperbaric oxygen. J Neurosurg Anesthesiol. 1995; 7:271–279. [PubMed: 8563448]

Shen Q, Meng X, Fisher M, Sotak CH, Duong TQ. Pixel-by-pixel spatiotemporal progression of focal ischemia derived using quantitative perfusion and diffusion imaging. J Cereb Blood Flow and Metab. 2003; 23:1479–1488. [PubMed: 14663344]

Shen Q, Ren H, Cheng H, Fisher M, Duong TQ. Functional, perfusion and diffusion MRI of acute focal ischemic brain injury. J Cereb Blood Flow and Metab. 2005; 25:1265–1279. [PubMed: 15858531]

Sicard KM, Duong TQ. Effects of Hypoxia, Hyperoxia and Hypercapnia on Baseline and Stimulus-Evoked BOLD, CBF and CMRO2 in Spontaneously Breathing Animals. Neuroimage. 2005; 25:850–858. [PubMed: 15808985]

Stamler JS, Jia L, Eu JP, McMahon TJ, Demchenko IT, Bonaventura J, Gernert K, Piantadosi CA. Blood flow regulation by S-nitrosohemoglobin in the physiological oxygen gradient. Science. 1997; 276:2034–2037. [PubMed: 9197264]

Ugurbil K, Adriany G, Andersen P, Chen W, Gruetter R, Hu X, Merkle H, Kim DS, Kim SG, Strupp J, Zhu XH, Ogawa S. Magnetic resonance studies of brain function and neurochemistry. Annu Rev Biomed. 2000; 2:633–660.

van Hulst RA, Haitsma JJ, Klein J, Lachmann B. Oxygen tension under hyperbaric conditions in healthy pig brain. Clin Physiol Funct Imaging. 2003; 23:143–148. [PubMed: 12752556]

Whalen RE, Saltzman HA, Holloway DH Jr, McIntosh HD, Sieker HO, Brown IW Jr. Cardiovascular and Blood Gas Responses to Hyperbaric Oxygenation. Am J Cardiol. 1965; 15:638–646. [PubMed: 14285147]

Xu F, Liu P, Pascual JM, Xiao G, Lu H. Effect of hypoxia and hyperoxia on cerebral blood flow, blood oxygenation, and oxidative metabolism. J Cereb Blood Flow Metab. 2012; 32:1909–1918. [PubMed: 22739621]
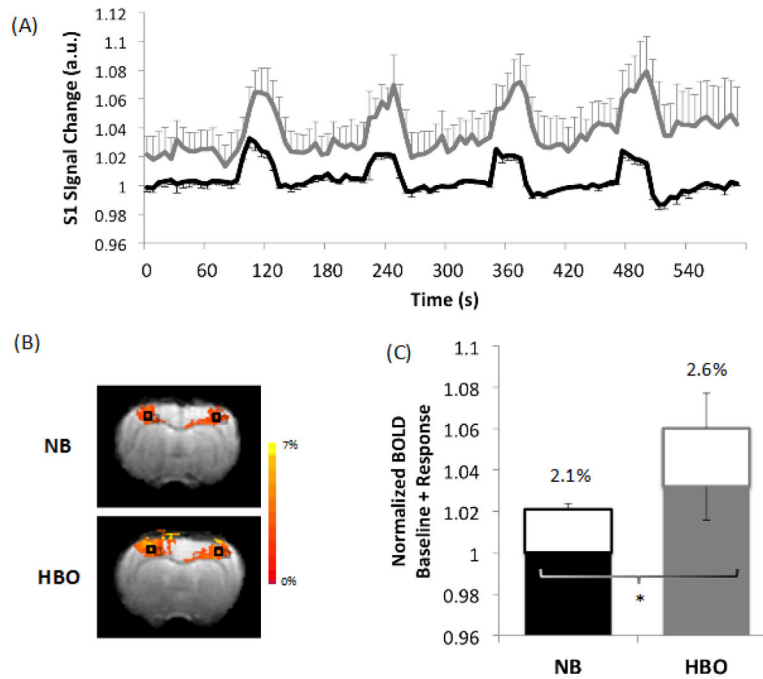
Figure 1.
BOLD fMRI under normobaric (NB) and 3ATA hyperbaric (HBO) conditions. (A) Normalized intensity time courses before and during forepaw stimulation under NB (black) and HBO (grey) conditions (Mean ± SEM for N = 8). (B) BOLD activation maps with overlaid representative ROIs under NB and HBO conditions from one animal. (C) Normalized baseline and evoked response changes in BOLD (normalized to baseline NB values) to an evoked response during normobaric air (NB) and hyperbaric oxygen (HBO) conditions. Mean ± SEM for N = 8. Baseline T_2^*-weighted signals were statistically different between NB and HBO as indicated by * P < 0.05. There were however no statistically significant differences in stimulus-evoked BOLD percent changes between the NB and HBO conditions.
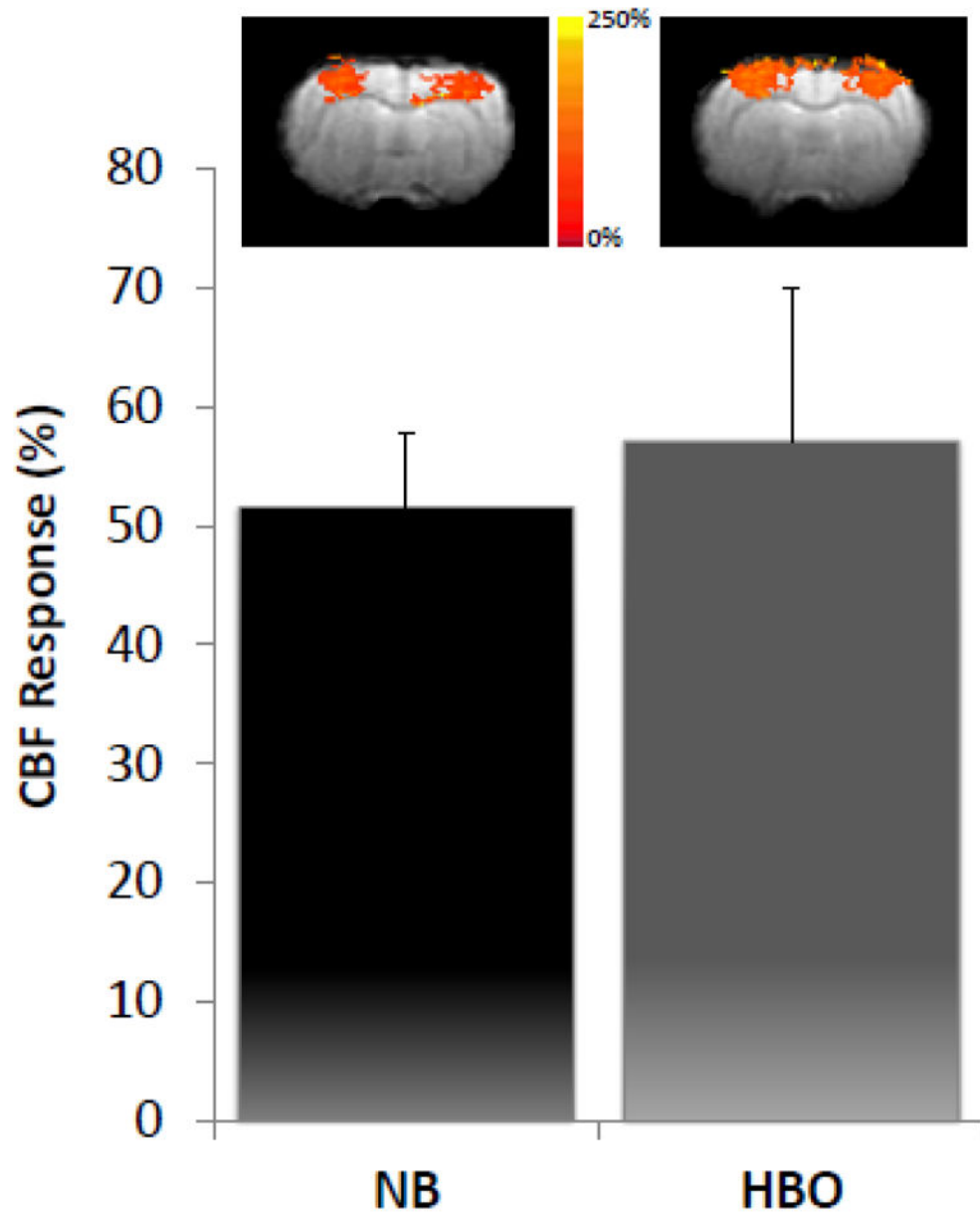
Figure 2.
CBF fMRI under NB and 3ATA HBO showing activation maps and percent change to an evoked response. Activation maps are from a single representative animal. Mean ± SEM for N = 8. There were no statistically significant differences between the NB and HBO conditions.
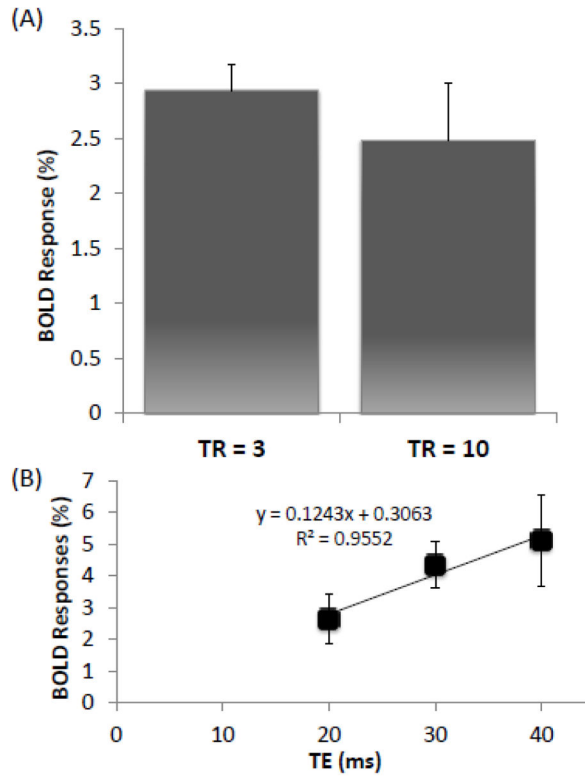
Figure 3.
(A) Evoked BOLD response during HBO in the somatosensory cortices using different repetition times (TR). (B) Evoked BOLD response during HBO in the somatosensory cortices using different echo times. The solid line is calculated trend-line for evoked BOLD response to different echo times. ROI's are located on the S1 region. Mean ± SEM for N = 3. There were no statistically significant differences between the two TRs. The percent change, extrapolated to echo time = 0 ms, was not significantly different from baseline (0 percent change).
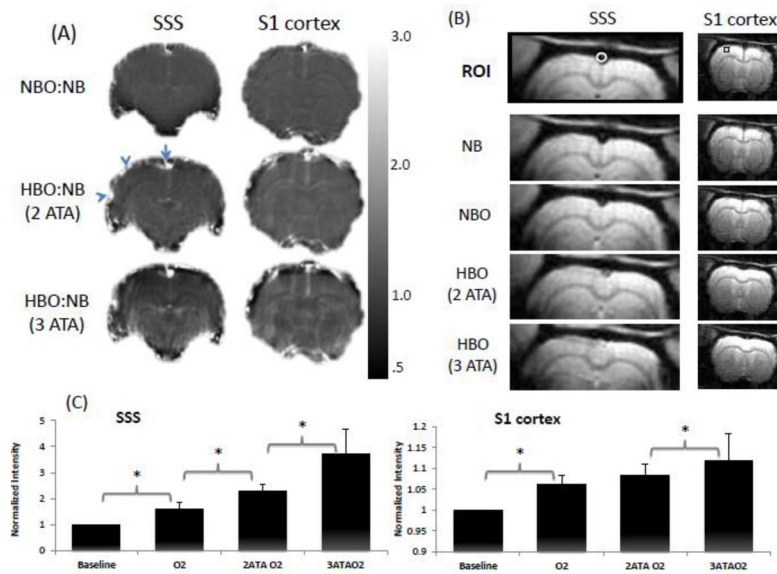
Figure 4.
(A) Ratio images relative to NB of NBO, 2ATA HBO, and 3ATA HBO. NB: normbaric air, NBO: normobaric oxygen, ATA: atmospheres absolute, HBO: hyperbaric oxygen. Two slices are shown for the SSS and S1 regions. (B) Signal intensity change in the superior sagittal sinus (SSS) and somatosensory cortex during pressurization. ROIs are indicated for the SSS (white) and the S1 region (black). (C) Intensity changes in the SSS and S1 region were normalized to their respective NB values. Mean ± SEM for N = 3. All conditions are significantly different from each other (* $P < 0.05$), except between the increase from normobaric oxygen (O_2) to 2ATA HBO in the S1 (P=0.056).
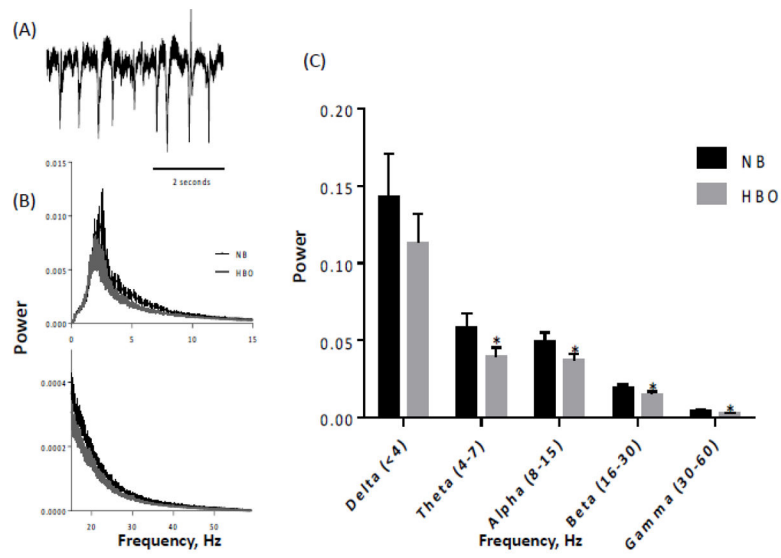
Figure 5.
Power spectrum of spontaneous electrophysiological recordings under HBO and NB. (A) Typical recording of spontaneous activity. (B) Power spectrum from 0–15 and 15–60 Hz. (C) Power spectrum separated into different frequency bands. Mean ± SEM for N = 8, * P < 0.05 from NB.
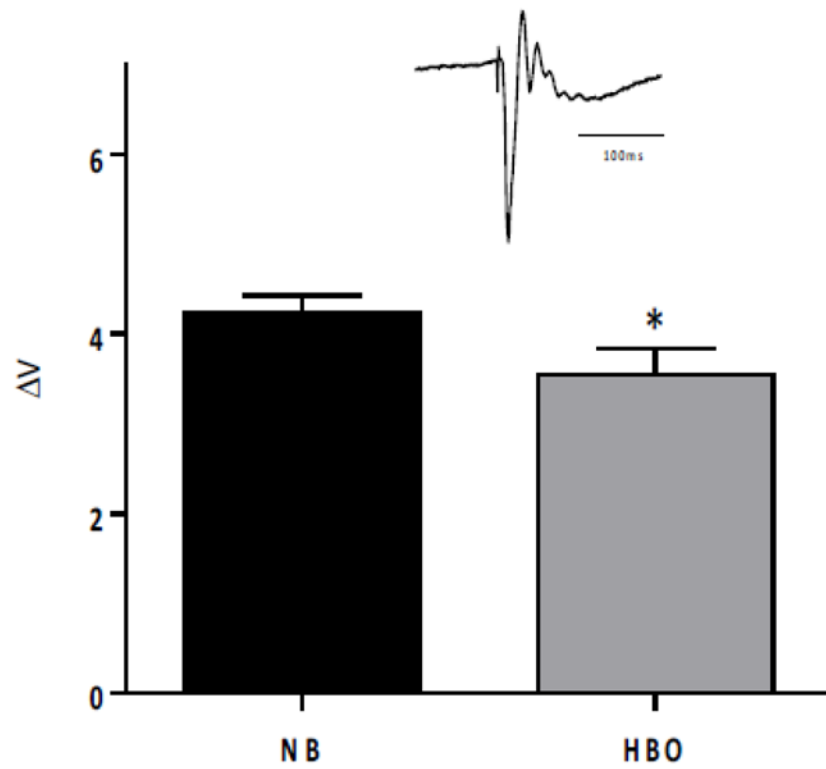
Figure 6.
Local field potential in the S1 somatosensory cortex following forepaw stimulation during NB and HBO. The inset shows a typical evoked potential. Mean ± SEM for N = 7, * P < 0.05.

Table 1

Physiological Measurements (mean ± SEM, n = 11 out of 22).

	NB	HBO
Respiration rate (brpm)	73.4 ± 4.6	56.3 ± 6.3[*]
Heart rate (bpm)	375 ± 43	360 ± 39
O_2 saturation (%)	93.6 ± 3.1	99.0 ± 0.6[*]

[*] indicates significant difference from NB (p<0.05).